International Journal of Renewable Energy Technology Research
Vol. 4, No. 6, December 2015, pp. 1-19, ISSN: 2325 - 3924 (Online)
Available online at http://ijretr.org

**Research article**

# Parametric analysis and optimization of a new combined power and refrigeration cycle using intermediate throttling and condensing stages

**HosseinRezvantalab[a,*] and AbdolrezaFazeli[b]**

[a]Department of Chemical Engineering, University of Michigan, NCRC, Biointerfaces Institute, Ann Arbor, MI 48109, USA, Tel: +1-732-277-4631, E-mail: rezvan@umich.edu

[b]Department of Mechanical and Aerospace Engineering, University of Florida, Gainesville, FL 32611, USA, Tel: +1-352-871-6389,E-mail: abfazeli@ufl.edu

*Corresponding author, Fax: +1-734-763-7924



---

## Abstract

A new combined power and refrigeration cycle using ammonia-water mixture as the working fluid is proposed, which employs two independent turbines and one cooling heat exchanger to produce both power and refrigeration output simultaneously, using only one heat source. A feed-forward neural network is used to simulate the thermodynamic properties of the working mixture and the relationship between the input parameters and the cycle performance. It is shown that the turbine inlet pressure, heat source temperature, and recovery heat exchanger mass flow rate ratio have contradictory effects on the net power and refrigeration outputs, as well as the exergy efficiency of the combined cycle. A multi-objective genetic algorithm (GA) is used for Pareto approach optimization of the cycle, based on second law efficiency and refrigeration load as the objective functions. Pareto fronts indicate that the combined cycle can provide a maximum exergy efficiency of

83% when the refrigeration load is only 100 kW. Otherwise, a cooling output as high as 600 kW can be achieved if a lower efficiency of 63% is satisfactory. 

**Keywords**: combined cycle; ammonia-water mixture; throttling stage; multi-objective Pareto optimization

---

## 1. Introduction

Currently, two-thirds of the world's electricity demand is met by non-renewable fossil fuels which has led to serious environmental problems and a widespread energy crisis. In an attempt to limit the emissions from the electricity generating sector, new energy resources should be developed. A variety of solutions for utilizing renewable energy (such as geothermal sources and solar energy) and waste heat (including exhaust gas from turbines and engines or hot water from industrial plants) have been proposed in the literature [1-6]. Among these solutions, the use of multi-component working fluids has gained significant attention in recent years. Binary mixtures exhibit a variable boiling temperature during the boiling process and keep a relatively constant temperature difference between them and variable temperature heat sources, which leads to reduced-exergy losses in the heat addition process. The ammonia–water mixture is a widely-used binary mixture, which not only has excellent thermo-physical properties, but also is an environmentally-friendly material.

A topic of recent interest is the idea of combined power and cooling cycles that use an ammonia-water working fluid for simultaneous power generation and refrigeration using a low temperature heat source. The cited advantages of combined operation include a reduction in capital equipment by sharing of components, as well as the possibility of improved resource utilization compared to separate power and cooling systems[7, 8]. A combined thermal power and refrigeration cycle was proposed by Goswami[9] using very high concentration ammonia vapor in the turbine which could be expanded to a very low temperature in the turbine without condensation. Further researches have focused on improving the cycle performance and analyzing the efficiency over a range of heat source temperatures for various applications[10-19]. Although this cycle could provide considerable power output as well as refrigeration load and utilized an absorption condensation instead of the conventional condensation process, it had a major shortcoming. Employing the ammonia-rich vapor in the turbine to generate power resulted in a relatively small refrigeration output. Zheng et al. [20] proposed a combined power/cooling cycle utilizing Kalina's technology. They replaced the flash tank in Kalina cycle with a rectifier, which could obtain a higher concentration ammonia-water vapor for refrigeration. Moreover, a

condenser and an evaporator were inserted between the rectifier and the second absorber. Considerable improvement in power and refrigeration outputs could be achieved by these adjustments. In a similar work, a parallel mode cycle was developed, combining an ammonia-water Rankine cycle and an ammonia refrigeration cycle, interconnected by absorption, separation and heat transfer processes [21]. The effects of the critical thermodynamic parameters on both energy and exergy efficiencies were investigated. More recently, exergy analysis of a combined power and cooling cycle was performed to determine the influence of pressure ratio, ammonia mass fraction at the absorber, and turbine efficiency on the total exergy destruction of the cycle [19]. It was demonstrated that the presence of the superheater after the rectification process reduces the exergy destruction of the cycle at high turbine efficiency values.

Optimization of engineering designs has always been of great importance and interest particularly in solving convoluted and practical design problems. In thermal systems, there are many complex optimization design problems in which the objectives can be conflicting and non-commensurable [22]. Recently, optimization of combined power and refrigeration systems has received much attention as a result of the growing concern about the deficiency in non-renewable energy resources and industrial pollution. Several studies have provided parametric analyses to optimize the operating conditions for achieving maximum power, refrigeration load, or second law efficiency [23-28]. Multi-objective GA algorithm has been applied with Pareto approach for optimization of a combined power/cooling cycle using the results of thermodynamic performance of a previously proposed cycle for optimization purposes [29].The multi-objective optimization led to discovery of important relationships among some objective functions and design variables, which can be used as useful optimal design principles.

In this study, we propose a novel power and refrigeration cycle operating in a parallel mode combining ammonia-waterRankine and ammonia refrigeration cycles. Two major improvements are introduced upon typical combined cycles. Firstly, the rectified vapor leaving the superheater is expanded to a mid pressure in the turbine, then fed to a condenser and throttled to the cycle low pressure before entering the refrigeration heat exchanger. This leads to an enhanced refrigeration output compared to relatively small load extracted from the originally developed cycle [10]. Secondly, the stream entering the recovery heat exchanger gets heat using the external heat source. Consequently, the hot weak solution exiting the boiler is combined with the rectified liquid and fed into a second superheater, providing some extra output work. The main objective of the present work is to investigate the effect of key thermodynamic parameters on the cycle performance and to define the optimum working conditions based on a set of specified assumptions. A neural network is proposed and trained in order

to evaluate the cycle outputs in the whole acceptable range of pre-defined input parameters. The cycle is then optimized using multi-objective GA algorithm for maximum exergy efficiency and refrigeration load.

## 2. CycleModeling and Optimization Procedure

### *2.1 Cycle description and assumptions*

The proposed cycle is a combination of Rankine and the absorption refrigeration cycles, which is capable of producing both power and refrigeration simultaneously using only one heat source. We quantify the exergy efficiency and the refrigeration load of the cycle in order to show the advantages of this novel design over the previous cycles. Exergy efficiency has proven to be a reliable parameter for representing the effectiveness of thermodynamic systems and has been quantified in most relevant studies. On the other hand, improving the refrigeration load is a key issue in cooling thermodynamic cycles and is thus considered as the second main objective of the current analysis.

By definition, exergy efficiency is a measure of the maximum extractable work from a system (operating under a set of thermodynamic constraints) with respect to a reference state. This reference state (also known as dead state) is arbitrary, but commonly defined such that it reproduces the environment of the system with zero work potential. As such, we consider the dead state in our analysis as the state in which the thermodynamic properties of the working fluid are equivalent to those of the environment around the system.

A schematic representation of the proposed cycle is shown in Figure 1. At state 1, the saturated solution leaving the absorber with basic concentration is assumed to be at a fixed absorber temperature (assumed 300 K here) and maintaining the cycle's low pressure $P_{low}$. A pump is then used to increase the pressure of the saturated liquid to the cycle's high pressure limit $P_{high}$(state 2). At this point, the high pressure liquid is divided into two streams: a portion passes through the rectifier, while the rest is directed towards a recovery heat exchanger where it gains heat from the hot fluid leaving the boiler and is consequently mixed with the first stream leaving the rectifier. The mixture is then directed into the boiler (state 4), where it is partially boiled, yielding a two-phase fluid composed of a vapor with high ammonia concentration and a weak liquid solution. The vapor is condensed in the rectifier, such that its ammonia content reaches x = 1 at rectifier temperature (state 7). The temperature of this rectified vapor is subsequently increased in the first superheater, and is then expanded through a turbine to an intermediate pressure $P_{mid}$. The fluid leaving the turbine is cooled down in a condenser and throttled back to the cycle's low pressure, while reaching a temperature lower than that of the ambient. This

allows the extraction of a significant refrigeration (cooling) load from the pure ammonia liquid as it enters the refrigeration heat exchanger (state 17).

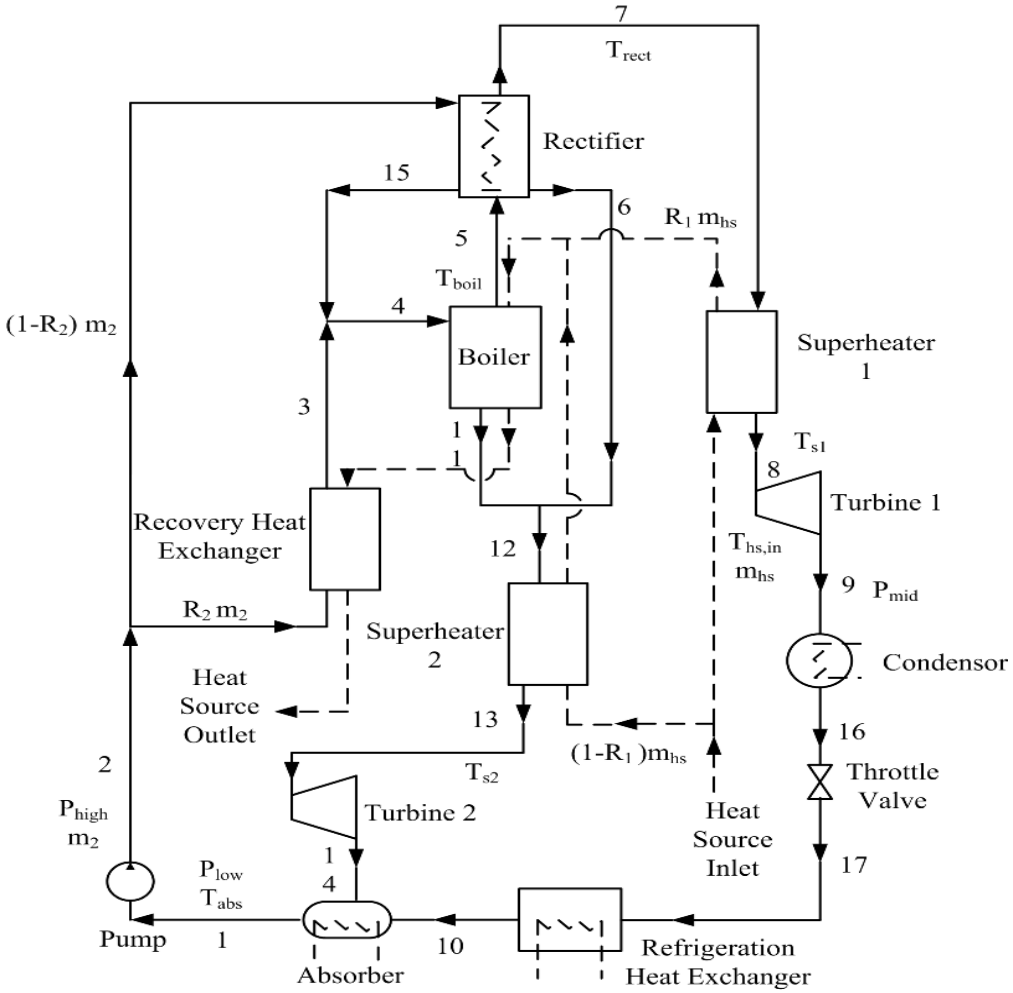


**Figure 1. Schematic diagram of the combined power and refrigeration cycle**

The other stream leaving the boiler containing a hot weak solution (state 11) is mixed with the rectified saturated liquid (state 6) and directed towards the second superheater, where it is heated up to $T_{s2}$. Consequently, the superheated mixture is expanded through a second turbine back to the cycle's low pressure $P_{low}$. The inclusion of the second turbine is thus advantageous as it enables the extraction of additional output work from the fluid that does not contribute to the refrigeration load. Finally, the weak ammonia solution extracted from the second turbine (state 14) is fed into an absorber, where it is added to the high concentration ammonia mixture leaving the refrigeration heat exchanger which has supplied the cooling load. This completes the cycles as the solution is condensed until returning to the specified absorber temperature, while maintaining the cycle's low pressure.

In order to provide the heatrequired in superheaters, boiler, and the recovery heat exchanger, we employ an external heat source composed of an air stream for which the entrance temperature is controlled in the range of 500-580 K. The cycle's mid pressure is assumed to be equal to 0.6 $P_{high}$, while $P_{high}$ is varied from 10 to 35 bars. The recovery heat exchanger mass flow rate ratio $R_2$is varied in the range of 0.1 to 0.9 to examine its influence on the performance of the combined cycle. We neglect the pressure drops and heat losses in pipelines as well as the work required by the pump to pressurize the saturated liquid solution leaving the absorber. The exit temperatures from both superheaters are assumed to have a pinch-point temperature difference of $T_{pp}$=35˚C with respect to the heat source inlet temperature. The major assumptions used in our analysis are summarized in Table 1.

**Table 1. Conditions assigned to the cycle parameters**

| | |
|---|---|
| Environment temperature (K) | 300 |
| Environment pressure (bar) | 1 |
| Absorber outlet temperature (K) | 300 |
| Refrigeration temperature (K) | 260 |
| Pinch point temperature difference (K) | 35 |
| Working mixture mass flow rate (kg/s) | 1 |
| Heat source mass flow rate (kg/s) | 14 |
| Heat source mass flow rate ratio $R_1$ | 0.5 |
| 1st Turbine isentropic efficiency (%) | 80 |
| 2nd Turbine isentropic efficiency (%) | 85 |
| Pump isentropic efficiency (%) | 100 |
| The range of turbine inlet pressure (bar) | 10-35 |
| The range of heat source inlet temperature (K) | 500-580 |
| The range of recovery heat exchanger mass flow rate ratio $R_2$ | 0.1-0.9 |

## *2.2 Artificial neural network*

Determining the thermodynamic properties of ammonia–water mixture, which has significant effect on the performance of the cycle, as well as analyzing thermodynamic characteristics of the combined power and cooling system usually require a large amount of computational power and time. The former is presented in literature as limited experimental data or complex differential equations and the latter is too complex because it involves the solution of complex differential equations [30-33].

Instead of solving complex equations and applying limited experimental data, faster and simpler solutions can be obtained using artificial neural networks (ANNs).

ANNs are useful tools in learning key information patterns within complex systems and therefore have been extensively used in simulating and predicting properties of fluid components in the last decade [34-40]. One of the major advantages of ANNs is that they can be trained just by using examples hence do not require a numerical formulation of physical relationships.

A typicalartificial neural network system is made of three types of layers, an input layer, a hidden intermediate layer made up of points (artificial neurons) that links the data taken from the input layer to the output layer, and an output layer that delivers the final results. Using a suitable learning method, ANNs are trained in order to find the optimum relation between the input data and output data while minimizing the error between the network output and desired output. The trained network can then be used to predict the system outputs for the new and unknown inputs. In this study, a neural network with two intermediate layers is used to simulate the thermodynamic properties of ammonia-water mixture. Additionally, another ANN is employed to simulate the relationship between the input thermodynamic parameters on the cycle performance. There are ten and nine in the first and second hidden layer, respectively.

The ANN used in this study is trained based on a back-propagation (BP) training scheme. This algorithm is a gradient descent method, in which the network weights are changed along the negative of the gradient of the performance function. It has been shown that networks that have been trained based on BP algorithm can minimize the error if properly trained [41].

### *2.3 Optimization technique*

To design an optimal combined power and refrigeration cycle, one needs to consider not only the second law efficiency of the cycle itself, but also the design constraints. These include the maximum possible pressure of the feed-water at the outlet of the pump, the minimum acceptable refrigeration load, as well as turbine's work, heat exchangers efficiency, size of condenser, and manufacturing cost. In view of achieving an optimal cycle, most of the above design variables have mutual effect on each other. For instance, high pressure feed-water at pump outlet can be viewed as an effective way to improve the thermal efficiency; however, this also leads to lower refrigeration load which may lie outside the acceptable range.

A multi-objective optimization problem is generally solved for a vector function *f*, which maps a vector of parameters, *z*, to a vector of goals, *y*, *constrained to a set of boundary conditions*, *h*. As a result, the optimization problem can be stated as:

$$optimizey = f(z) = (f_1(z), f_2(z), \dots, f_n(z)) \quad (1)$$

$$subjecttoh(z) = (h_1(z), h_2(z), \dots, h_n(z)) \leq 0 \quad (2)$$

The two objective functions considered in this study are the exergy efficiency and the refrigeration load of the cycle. The goal is to maximize both objective functions, through variation of a set of three input parameters, which pose the initial optimization problem as follows:

$$Maxf_1(z_1, z_2, z_3): Exergyefficiency \quad (3)$$

$$Maxf_2(z_1, z_2, z_3): Refrigerationload \quad (4)$$

Parameters:

$$z_1: Turbineinletpressure \quad (5)$$

$$z_2: Heatsourceinlettemperature \quad (6)$$

$$z_3: recoveryheatexchangermassflowrateratio \quad (7)$$

The solution of equations (3,4) is usually not unique, but a set of equally efficient, non-dominated solutions, known as Pareto-optimal set [35].

Following the concept of Pareto optimality, the solutions searched must have the characteristic that it is not possible to increase cycle exergy efficiency without decreasing refrigeration load simultaneously or, in other words, it is not possible to increase the refrigeration load without decreasing exergy efficiency at the same time.

There are several approaches to solve a multi-objective optimization problem. One of the easiest ways is to optimize a single aggregate objective function (AOF). In this approach, all the objective functions will be weighted and then added together to form a single objective function. The final function is then optimized using one of the common objective methods.

Solving several AOFs, made from different weighting functions, is another way of solving multi-obective functions. Although this method has great advantage over single AOF method, it still can't be applied to complicated problems. Recently, utilization of evolutionary algorithms such as particle swarm optimization (PSO) [42]and Genetic Algorithm (GA) [36] in solving multi-objective optimization processes has received significant attention since it is shown that they can find the Pareto-optimal set with maximum accuracy. The most widely used method to solve multi-objective optimization problems is to apply Genetic Algorithm because

there is no need to linearize the problem or calculate partial derivatives when finding the optimized results. The constrained optimization problem in the present study is solved by the multi-objective GA method.

## 3. Results and Discussion

### *3.1 Evaluation of the employed artificial neural network*

As mentioned previously, a feed-forward neural network with two hidden layers is employed to model the cycle performance based on the above input variables. In order to achieve accurate results while decreasing the calculation time as much as possible, several networks have been trained and their relative errors associated with second law efficiency, as well as their respective training calculation times were compared. To find the most suitable network, the effects of number of neurons at each hidden layer on the mentioned parameters have been investigated. An exhaustive search method was applied to find the best values of neurons at each level which lead to the most fitting network, and the result is shown in Table 2.The first line indicates the optimum choice of neuron numbers for training the neural network, in order to predict the cycle performance. It can be seen that both normalized calculation time and relative error of the optimum network is smaller than the other ones with different number of neurons listed in other rows of the Table. We conclude that a network with two hidden layers, containing ten and nine neurons in the first and second hidden layers respectively, shows the best result in predicting the cycle performance.

**Table 2. Normalized values of calculation time and efficiency error in different neuron numbers for two hidden layers of examined ANN**

| *Number of neurons in the 1st layer* | *Number of neurons in the 2nd layer* | *Normalized Calculation Time* | *Normalized Relative Error* |
|---|---|---|---|
| **10** | **9** | **1.00** | **1.00** |
| 9 | 7 | 1.36 | 1.04 |
| 10 | 4 | 1.07 | 1.08 |
| 4 | 3 | 4.14 | 1.86 |
| 10 | 5 | 1.08 | 1.09 |
| 8 | 3 | 1.24 | 1.50 |

### *3.2 Parametric analysis of cycle performance*

A parametric analysis is performed to evaluate the effects of three major parameters on the combined cycle performance: turbine inlet pressure, heat source inlet temperature, and the recovery heat exchanger mass flow rate ratio $R_2$. When one specific parameter is studied, other parameters are kept constant.

The two objective functions are the exergy efficiency and the refrigeration load of the cycle, which can be defined as follows with respect to the states indicated in Figure 1:

$$\eta_{II} = \frac{m_7(h_8-h_9)+m_{12}(h_{13}-h_{14})+m_7[(h_{17}-h_{10})-T_0(s_{17}-s_{10})]}{m_{air}\,[c_{p,air}\,(T_{in,air}-T_0)-T_0 c_{p,air}\,ln(T_{in,air}/T_0)]} \qquad (8)$$

$$Q_{ref} = m_7(h_{10}-h_{17}) \qquad (9)$$

These functions implicitly depend on the three specified parameters, namely turbine inlet pressure, heat source inlet temperature, and the recovery heat exchanger mass flow rate ratio $R_2$. The thermodynamic considerations regarding the water-ammonia mixture impose some limitations on different states of the cycle. It should be noted that increasing one of the objective functions results in a reduction of the other one. So, a multi-objective technique should be employed in order to optimize the cycle performance.

**Table 3. Operating conditions of the combined cycle at $P_{high}$=20 bar, $T_{in}$=530 K, $R_2$=0.7**

| *state* | *P (bar)* | *T (˚C)* | *h (kJ/kg)* | *s (kJ/kg.K)* | *m (kg/s)* | *x* |
|---|---|---|---|---|---|---|
| 1 | 1 | 27 | -71.042 | 0.25775 | 1 | 0.30510 |
| 2 | 20 | 27.1 | -70.608 | 0.25935 | 1 | 0.30510 |
| 3 | 20 | 158.8 | 864.89 | 2.75907 | 0.7 | 0.30510 |
| 4 | 20 | 181.9 | 1504.11 | 4.41867 | 1 | 0.30510 |
| 5 | 20 | 195.0 | 2433.90 | 6.19811 | 0.7 | 0.30510 |
| 6 | 20 | 195.0 | 801.42 | 2.3397 | 0.18432 | 0.05674 |
| 7 | 20 | 49.3 | 1470.49 | 4.76460 | 0.51568 | 1 |
| 8 | 20 | 242.0 | 1822.80 | 5.36100 | 0.51568 | 1 |
| 9 | 12 | 196.4 | 1716.80 | 5.36099 | 0.51568 | 1 |
| 10 | 1 | -13 | 1262.92 | 5.30832 | 0.51568 | 1 |
| 11 | 20 | 195.0 | 2433.90 | 6.19811 | 0.3 | 0.30510 |
| 12 | 20 | 195.0 | 1812.63 | 4.85162 | 0.48432 | 0.21058 |
| 13 | 20 | 242.0 | 2657.88 | 6.51587 | 0.48432 | 0.21058 |
| 14 | 1 | 91.9 | 2091.76 | 6.51587 | 0.48432 | 0.21058 |
| 15 | 20 | 181.9 | 1517.16 | 4.41871 | 0.3 | 0.30510 |
| 16 | 12 | 30.8 | 324.916 | 1.20842 | 0.51568 | 1 |
| 17 | 1 | -33.5 | 324.9164 | 1.157761 | 0.515683 | 0.181993 |

For a turbine inlet pressure of 20 bar, heat source temperature of 550 K, and recovery heat exchanger mass flow rate ratio of $R_2$=0.7, operating conditions obtained from the thermodynamic simulation are shown in Table 3. The states indicated in the table correspond to locations given in cycle schematic in Figure 1. It is obvious that the temperatures of states 8 and 13 (which are defined by superheater temperatures) are equal to $T_{hs,in}$-$T_{pp}$, where

$T_{hs,in}$ is the heat source inlet temperature and $T_{pp}$ is the pinch point temperature difference at each superheater. On the other hand, the refrigeration temperature (state 10) corresponds to $T_0$-40. The boiler and rectifier temperatures are also obtained by using their two known thermodynamic properties: pressure and ammonia concentration.

**Table 4. The performance of the combined power and refrigeration cycle at $P_{high}$=20 bar, $T_{hs,in}$=530 K, $R_2$=0.7**

| | |
|---|---|
| Turbine 1 work (kW) | 43.7 |
| Turbine 2 work (kW) | 233.1 |
| Pump work (W) | 434.2 |
| Net power output (kW) | 276.4 |
| Refrigeration output (kW) | 356.7 |
| Net power and refrigeration output (kW) | 733.1 |
| Heat input (kW) | 1539.6 |
| Thermal efficiency (%) | 47.6 |
| Exergy efficiency (%) | 45.4 |

Moreover, it can also be observed that nearly half of the basic solution returns from the boiler to the absorber through the secondary superheater and turbine. In this case, about 52% of the basic solution is directed from the rectifier towards the primary turbine and refrigeration heat exchanger as pure ammonia, enabling the extraction of power and refrigeration load. Therefore, the employment of the second turbine seems essential for making use of considerable amount of available exergy from the hot weak solution leaving the boiler.

The results indicating the overall performance of the cycle are shown in Table 4. It is found that in this particular case, the refrigeration output is nearly 75% greater than the net power output. In addition, the insertion of the secondary turbine is beneficial in making use of the available exergy from the hot weak solution leaving the boiler that resulted in increasing the second law efficiency from 22.6% to 45.4%.

Figure 2(a) shows the effect of turbine inlet pressure on the net power output for different recovery heat exchanger mass flow rate ratios. The curves correspond to a pressure range of 10-35 bar and four different $R_2$ values, while the heat source inlet temperature is kept constant at $T_{hs,in}$=530 K. The markers indicate the values obtained by direct numerical solution, while the lines represent the results predicted by the neural network. It is evident that the power output increases by raising the cycle high pressure. It is known that the enthalpy drop across the turbine increases as its pressure ratio is increased. Since $P_{mid}$ is set to 0.6 $P_{high}$, and therefore is only a function of the cycle high pressure, the pressure ratio of the second turbine increases directly with $P_{high}$. Hence, a higher enthalpy drop occurs across both turbines and therefore, the working capacity of the cycle is considerably increased. On the other hand, it can be seen that increasing $R_2$ leads to a decrease in the output

work. Increasing the mass flow rate of the working fluid passing through the recovery heat exchanger is construed as raising the flow rate of the vapor rich in ammonia entering the rectifier, thus increasing the output work derived from the first turbine. However, since $m_{11}=m_2-m_5$, less flow will reach the second turbine, leading to fewer available work. Noting that the enthalpy drop across the second turbine is significantly greater than that of the first turbine because of its higher pressure ratio, the decrease in latter work has the dominant effect, and as a result, the net power output tends to decrease considerably.

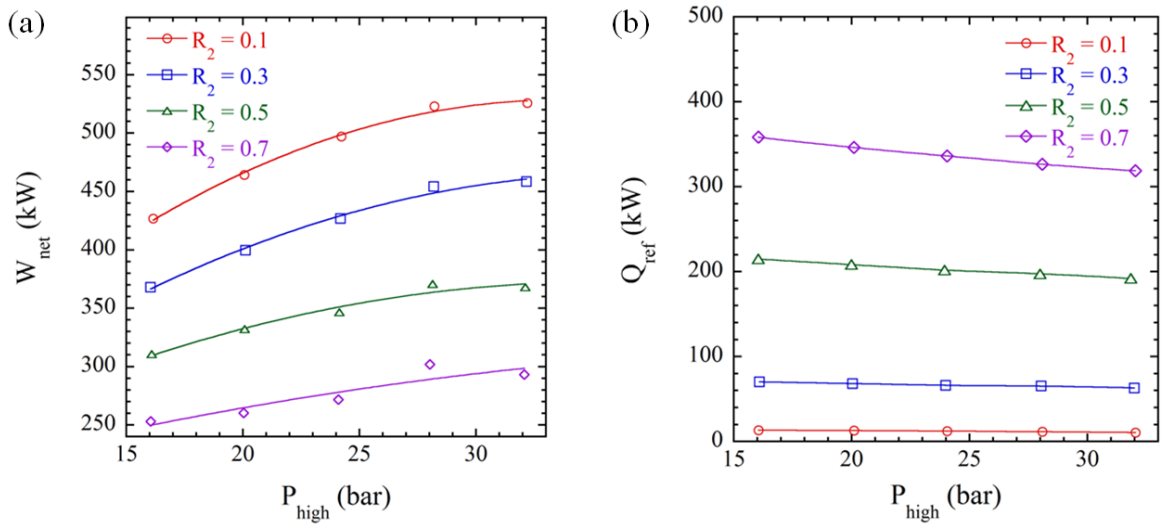


**Figure 2. Effect of turbine inlet pressure on (a) net power output and (b) the refrigeration output, for different recovery heat exchanger mass flow rate ratios $R_2$**

Figure2(b) demonstrates the effect of turbine inlet pressure on the refrigeration output for different recovery heat exchanger mass flow rate ratios $R_2$. The results are obtained for the same range of $P_{high}$, three different values of $R_2$, and a constant heat source temperature. It can be observed that the net refrigeration output generally drops as the turbine inlet pressure is increased. As the state of the working fluid exiting the refrigeration heat exchanger (point 10) is independent of the cycle's high pressure, the influence of this parameter on the state of the fluid entering the heat exchanger should be investigated. According to the previous discussion, a higher enthalpy drop occurs across the first turbine as its pressure ratio is increased, resulting in a lower enthalpy and temperature at the turbine exit. Assuming that the working fluid experiences a pressure-constant process in condenser until reaching the saturated liquid condition, a decreased mid temperature is identical to a lower saturated liquid enthalpy for the pure ammonia exiting the condenser. Since the subsequent throttling process is assumed to be enthalpy-constant, an increased enthalpy drop occurs across the refrigeration heat exchanger. However, as increasing the turbine inlet pressure reduces the mass flow rate passing through the recovery heat exchanger, the total refrigeration output reduces due to the prevailing effect of the lower flow rate.

Moreover, it is noticed that the cooling capacity of the cycle increases with recovery heat exchanger mass flow rate ratio $R_2$ in an approximately linear pattern, due to the increased mass flow rate of the rectified ammonia, reaching the refrigeration heat exchanger.

The effect of turbine inlet pressure on the exergy efficiency of the cycle is shown in Figure 3. It can be seen that due to the cumulative effects of net power output and refrigeration output on the performance of the combined cycle, the exergy efficiency increases first to maximum in proximity of $P_{high}$= 30 bar, and then decreases as the turbine inlet pressure is increased. Since the net power and refrigeration outputs exhibit inverse trends in response to the variation of turbine inlet pressure, the existence of a maximum for efficiency is reasonable. This indicates that at lower pressures, the output work has the dominant effect, whereas the decreasing trend of refrigeration output is prominent at higher pressures. Therefore, under each predefined set of input conditions, an optimum pressure may exist which maximizes the exergy efficiency of the cycle.

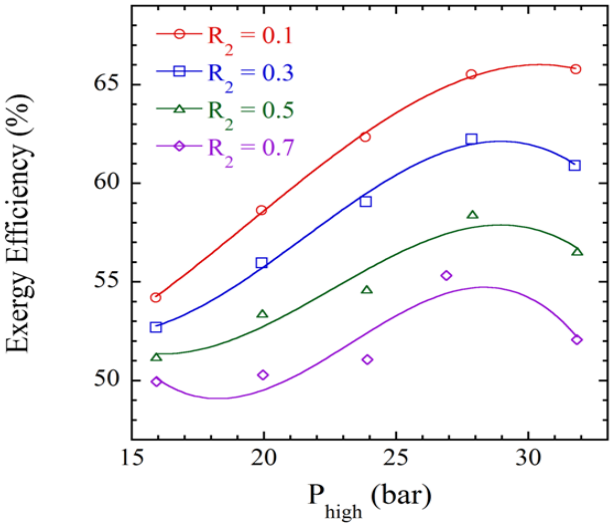


**Figure 3. Effect of turbine inlet pressure on exergy efficiency for different $R_2$**

Furthermore, the exergy efficiency generally decreases as the recovery heat exchanger mass flow rate ratio $R_2$ is increased. A comparison of the quantities reflected in Figure 2reveals that by increasing $R_2$, the decrease in the net power is more significant than the increase in refrigeration load. Therefore, their combined effect tends to deteriorate the efficiency. It is also evident that increasing $R_2$ will have a reverse impact on the performance of the cycle as the extracted mass should perform work at a lower pressure ratio; however, such approach is very appealing where there is a low temperature heat source available, *e.g.* geothermal energy.

Figure4(a) indicates the effect of heat source inlet temperature on net power output for different operating high pressures. The curves correspond to a heat source temperature in the range of 530-570 K and three different $P_{high}$ values, while the recovery heat exchanger mass flow rate ratio is kept constant at $R_2$=0.5. The values obtained by direct numerical solution are still specified by markers, while the lines represent the results predicted by the neural network. It can be observed that the net power output increases as the heat source inlet temperature is increased. This is because higher heat source temperature leads to higher turbine inlet temperature, thus raising the enthalpy drop across both turbines and enhancing the work capacity of the cycle.

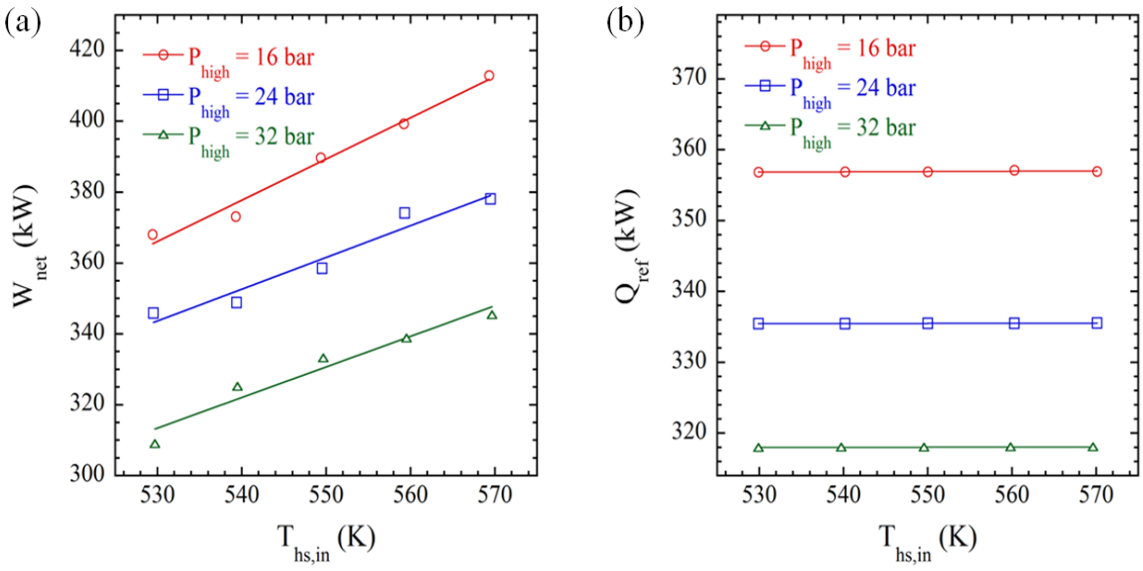


**Figure 4. The influence of heat source inlet temperature on (a) net power output and (b) the refrigeration output, for different $P_{high}$**

The effect of heat source inlet temperature on the refrigeration output is shown in Figure 4(b) for the same range of parameters. It is evident that the refrigeration output remains constant as the heat source temperature increases. This can be easily explained by considering that the inlet temperature of the refrigeration heat exchanger does not vary with the heat source temperature, and the outlet state is only a function of refrigeration temperature which is kept constant. Therefore, the heat source inlet temperature has no influence on the refrigeration output.

The influence of heat source inlet temperature on the exergy efficiency of the cycle is depicted in Figure 5. As it is observed, increasing the heat source temperature results in decreased exergy efficiency. Although increasing the heat source temperature leads to increased power output while the same rate of refrigeration is maintained, this enhancement occurs at the expense of inserting more exergy into the cycle. The trend indicates that the

amount of exergy that can be employed to produce useful power or refrigeration is negligible compared to the added input. Consequently, increasing the heat source temperature has a negative impact on the exergy efficiency of the cycle.

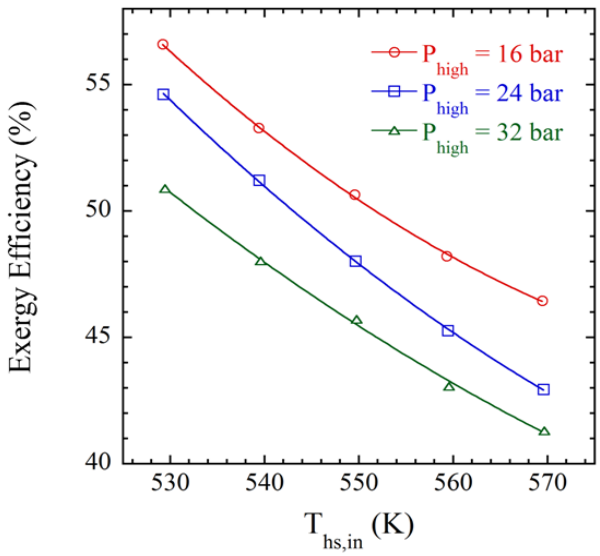


**Figure 5. Effect of heat source inlet temperature on exergy efficiency for different $P_{high}$**

In all previous figures, it is observed that the results derived from the trained network are in excellent agreement with the data obtained from direct numerical simulation. Moreover, from the discussions presented above, it can be concluded that the effects of three input parameters on the net power output, refrigeration output and exergy efficiency of the cycle are quite contradictory. In order to evaluate the performance of the combined power and refrigeration cycle, it is necessary to employ a multi-objective optimization method and define the optimum working conditions for the combined cycle.

### *3.3 Multi-objective optimization results*

Figure 6 shows the Pareto fronts related to the optimization case analyzed here. It can be observed that second law efficiencies as high as 83% are achievable at the expense of reducing the refrigeration load to ~100 kW. On the other hand, one may receive 600 kW of refrigeration load at the expense of reducing the second law efficiency to about 63%. As it was mentioned in the previous section, lowering heat source inlet temperature tends to increase the efficiency of the cycle while it has no sensible effect on refrigeration load. As a result, one may expect to reduce the heat source temperature in order to enhance the performance of the cycle.

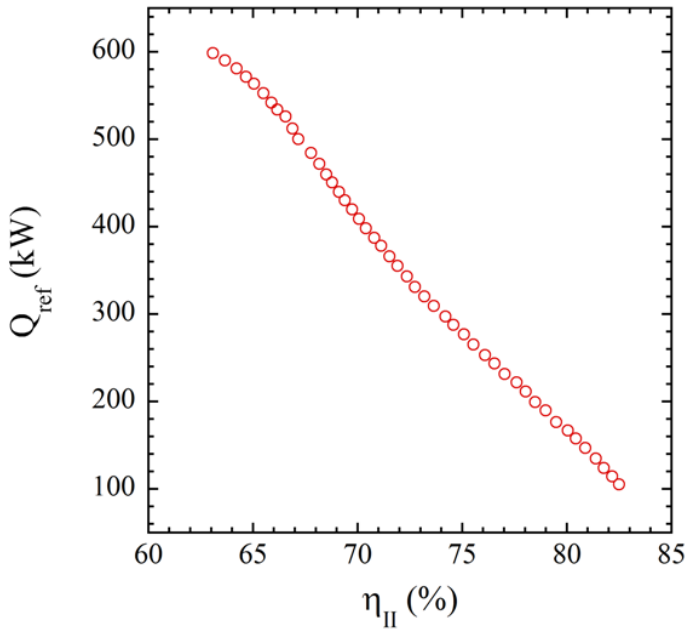


**Figure 6. Pareto Front for the optimization of Second law efficiency and Refrigeration Load**

## 4. Conclusions

A new combined power and refrigeration cycle using ammonia-water mixture as the working fluid is proposed, which combines the Rankine and absorption refrigeration cycles. Using a binary ammonia-water mixture as the working fluid, this combined cycle produces both power and refrigeration output simultaneously by employing one external heat source. In order to achieve the highest possible exergy efficiency, a secondary turbine is inserted to expand the hot weak solution leaving the boiler. Moreover, an artificial neural network is used to simulate the thermodynamic properties and the relationship between the input thermodynamic variables on the cycle performance. It is shown that turbine inlet pressure, heat source temperature, and recovery heat exchanger mass flow rate ratio have different effects on the net power and refrigeration outputs, as well as the exergy efficiency of the combined cycle. This parametric analysis of the cycle and the contradictory trends of output parameters based on input conditions showed the potential for the cycle to be optimized using a multi-objective method.

Pareto fronts are obtained for a particular case of optimization of thermal parameters by means of genetic algorithm, considering second law efficiency and refrigeration output as the objective functions. Significantly high efficiencies and refrigeration loads can be achieved by setting the input thermodynamic parameters to their proper values. It is demonstrated that the combined cycle can provide a maximum exergy efficiency of 83%

when the refrigeration load is 100 kW. On the other hand, refrigeration outputs as high as 600 kW can be extracted at the expense of reducing the exergy efficiency to 63%.

## References

1. D.Y. Goswami ,F. Xu, *Analysis of a new thermodynamic cycle for combined power and cooling using low and mid temperature solar collectors.* Journal of Solar Energy Engineering-Transactions of the Asme, 1999. **121**(2): p. 91-97.
2. W. Qiang, Y.Z. Li, W. Jiang, *Analysis of power cycle based on cold energy of liquefied natural gas and low-grade heat source.* Applied Thermal Engineering, 2004. **24**(4): p. 539-548.
3. S. Vijayaraghavan ,D.Y. Goswami, *A combined power and cooling cycle modified to improve resource utilization efficiency using a distillation stage.* Energy, 2006. **31**(8-9): p. 1177-1196.
4. C.J. Butcher ,B.V. Reddy, *Second law analysis of a waste heat recovery based power generation system.* International Journal of Heat and Mass Transfer, 2007. **50**(11-12): p. 2355-2363.
5. M. Liu ,N. Zhang, *Proposal and analysis of a novel ammonia-water cycle for power and refrigeration cogeneration.* Energy, 2007. **32**(6): p. 961-970.
6. X. Shi ,D. Che, *A combined power cycle utilizing low-temperature waste heat and LNG cold energy.* Energy Conversion and Management, 2009. **50**(3): p. 567-575.
7. D.C. Erickson, G. Anand, I. Kyung, *Heat-activated dual-function absorption cycle.* ASHRAE Transactions 2004. **110**(1): p. 515–524.
8. Y. Amano, et al., *A hybrid power generation and refrigeration cycle with ammonia–water mixture. IJPGC2000-15058.* Proceedings of 2000 Joint Power Generation Conference, ASME, 2000. **IJPGC2000-15058**.
9. F. Xu, D.Y. Goswami, S.S. Bhagwat, *A combined power/cooling cycle.* Energy, 2000. **25**(3): p. 233-246.
10. A.A. Hasan, D.Y. Goswami, S. Vijayaraghavan, *First and second law analysis of a new power and refrigeration thermodynamic cycle using a solar heat source.* Solar Energy, 2002. **73**(5): p. 385-393.
11. D.Y. Goswami, et al., *New and emerging developments in solar energy.* Solar Energy, 2004. **76**(1-3): p. 33-43.
12. G. Tamm, et al., *Theoretical and experimental investigation of an ammonia-water power and refrigeration thermodynamic cycle.* Solar Energy, 2004. **76**(1-3): p. 217-228.
13. A. Vidal, et al., *Analysis of a combined power and refrigeration cycle by the exergy method.* Energy, 2006. **31**(15): p. 3401-3414.
14. C. Martin ,D.Y. Goswami, *Effectiveness of cooling production with a combined power and cooling thermodynamic cycle.* Applied Thermal Engineering, 2006. **26**(5-6): p. 576-582.
15. S.M. Sadrameli ,D.Y. Goswami, *Optimum operating conditions for a combined power and cooling thermodynamic cycle.* Applied Energy, 2007. **84**(3): p. 254-265.
16. Y. Dai, J. Wang, L. Gao, *Exergy analysis, parametric analysis and optimization for a novel combined power and ejector refrigeration cycle.* Applied Thermal Engineering, 2009. **29**(10): p. 1983-1990.

17. G. Demirkaya, et al., *Analysis of a combined power and cooling cycle for low-grade heat sources.* International Journal of Energy Research, 2011. **35**(13): p. 1145-1157.
18. A. Khaliq, B.K. Agrawal, R. Kumar, *First and second law investigation of waste heat based combined power and ejector-absorption refrigeration cycle.* International Journal of Refrigeration-Revue Internationale Du Froid, 2012. **35**(1): p. 88-97.
19. A. Fontalvo, et al., *Exergy analysis of a combined power and cooling cycle.* Applied Thermal Engineering, 2013. **60**(1-2): p. 164-171.
20. D.X. Zheng, et al., *Thermodynamic analysis of a novel absorption power/cooling combined-cycle.* Applied Energy, 2006. **83**(4): p. 311-323.
21. N. Zhang ,N. Lior, *Development of a novel combined absorption cycle for power generation and refrigeration.* Journal of Energy Resources Technology-Transactions of the Asme, 2007. **129**(3): p. 254-265.
22. A. Bijan, G. Tsatsaronics, M. Moran, *Thermal and design optimization*. 1996, New York: Wiley.
23. S. Lu ,D.Y. Goswami, *Theoretical analysis of ammonia based combined power/ refrigeration cycle at lowrefrigeration temperatures.* Solar Engineering. ASME, 2002: p. 117–126.
24. S. Vijayaraghavan ,D.Y. Goswami, *On evaluating efficiency of a combined power and cooling cycle.* Journal of Energy Resources Technology-Transactions of the Asme, 2003. **125**(3): p. 221-227.
25. A. Cihan, O. Hacihafizoglu, K. Kahveci, *Energy-exergy analysis and modernization suggestions for a combined-cycle power plant.* International Journal of Energy Research, 2006. **30**(2): p. 115-126.
26. J. Wang, Y. Dai, L. Gao, *Parametric analysis and optimization for a combined power and refrigeration cycle.* Applied Energy, 2008. **85**(11): p. 1071-1085.
27. J. Wang, et al., *Parametric analysis for a new combined power and ejector-absorption refrigeration cycle.* Energy, 2009. **34**(10): p. 1587-1593.
28. H. Wang, X. Shi, D. Che, *Thermodynamic optimization of the operating parameters for a combined power cycle utilizing low-temperature waste heat and LNG cold energy.* Applied Thermal Engineering, 2013. **59**(1-2): p. 490-497.
29. M. Pouraghaie, et al., *Thermodynamic performance optimization of a combined power/cooling cycle.* Energy Conversion and Management, 2010. **51**(1): p. 204-211.
30. F. Xu ,D.Y. Goswami, *Thermodynamic properties of ammonia-water mixtures for power-cycle applications.* Energy, 1999. **24**(6): p. 525-536.
31. G. Soleimani Alamdari, *Simple equations for predicting entropy of ammonia-water mixture.* International Journal of Engineering 2007. **20**: p. 97-106
32. J. Patek ,J. Klomfar, *Simple functions for fast calculations of selected thermodynamic properties of the ammonia-water system.* International Journal of Refrigeration-Revue Internationale Du Froid, 1995. **18**(4): p. 228-234.
33. E. Thorin, *Thermophysical properties of ammonia-water mixtures for prediction of heat transfer areas in power cycles.* International Journal of Thermophysics, 2001. **22**(1): p. 201-214.
34. T.T. Chow, et al., *Global optimization of absorption chiller system by genetic algorithm and neural network.* Energy and Buildings, 2002. **34**(1): p. 103-109.

35. E. Arcaklioglu, *Performance comparison of CFCs with their substitutes using artificial neural network.* International Journal of Energy Research, 2004. **28**(12): p. 1113-1125.
36. A. Parlak, et al., *Application of artificial neural network to predict specific fuel consumption and exhaust temperature for a Diesel engine.* Applied Thermal Engineering, 2006. **26**(8-9): p. 824-828.
37. H.M. Ertunc ,M. Hosoz, *Artificial neural network analysis of a refrigeration system with an evaporative condenser.* Applied Thermal Engineering, 2006. **26**(5-6): p. 627-635.
38. S.A. Fazeli, H. Rezvantalab, F. Kowsary, *Thermodynamic analysis and simulation of a new combined power and refrigeration cycle using artificial neural network.* Thermal Science, 2011. **15**(1): p. 29-41.
39. D. Kumlutas, et al., *Investigation of design parameters of a domestic refrigerator by artificial neural networks and numerical simulations.* International Journal of Refrigeration-Revue Internationale Du Froid, 2012. **35**(6): p. 1678-1689.
40. H. Benli, *Determination of thermal performance calculation of two different types solar air collectors with the use of artificial neural networks.* International Journal of Heat and Mass Transfer, 2013. **60**: p. 1-7.
41. J. Leonard ,M.A. Kramer, *Improvement of the backpropagation algorithm for training neural networks.* Computers & Chemical Engineering, 1990. **14**(3): p. 337-341.
42. J. Kennedy ,R. Eberhart, *Particle swarm optimization.* Proceedings of IEEE International Conference on Neural Networks, 1995. **4**: p. 1942-1948.